

Seismic Fragility of a Single Pillar-Column Under Near and Far Fault Soil Motion with Consideration of Soil-Pile Interaction

Foudhil Lemsara

LGC-ROI, Department of Civil Engineering, Faculty of Technology, University of Batna 2, Algeria
f.lemsara@univ-batna2.dz
(corresponding author)

Tayeb Bouzid

LGC-ROI, Department of Civil Engineering, Faculty of Technology, University of Batna 2, Algeria
tayeb.bouzid@univ-batna2.dz

Djarir Yahiaoui

LGC-ROI, Department of Civil Engineering, Faculty of Technology, University of Batna 2, Algeria
d.yahiaoui@univ-batna2.dz

Belgacem Mamen

Department of Civil Engineering, Faculty of Science and Technology, University of Abbès Laghrou
Khenchela, Algeria
belgacem.mamen@univ-khenchela.dz

Mohamed Saadi

LGC-ROI, Department of Civil Engineering, Faculty of Technology, University of Batna 2, Algeria
m.saadi@univ-batna2.dz

Received: 10 October 2022 | Revised: 30 October 2022 | Accepted: 31 October 2022

ABSTRACT

The soil-structure interaction is a significant challenge faced by civil engineers due to the complexity potential in terms of seismic fragility evaluation. This paper presents a seismic fragility estimation of a single pier considering seismic ground motion types. Furthermore, sand type, pile diameter, pier height, and mass variation were considered to estimate their effect on the seismic fragility of the concrete pier. Incremental dynamic analysis was performed using a beam on a nonlinear Winkler foundation model. The analysis model condition compared near- and far-ground motion effects. Dynamic analysis and fragility assessment of the single-pier structure showed that low mass center produced less vulnerability of the concrete pier in the two cases of the sand type under near- and far-ground motions. The near and far earthquake simulations at complete failure probability had a difference of less than 5% when $0.65s < T_1 < 1s$ and $2.4 < T_1/T_2$, but the opposite was shown when $T_1 < 0.5s$ and $3 < T_1/T_2$ were present together.

Keywords-soil-pile-structure interaction; incremental dynamic analysis; BNWFmodel; ground motion types; seismic fragility

I. INTRODUCTION

Under seismic loading, liquefiable soil increases the seismic fragility of expansion bearing, piles, and embankment soil. The fragility of common components, such as columns, depends on the overlying liquefiable sand. The effect of soil strength for clay and sandy sites on the seismic performance of

skewed bridge components and its relation with the skew angle was studied in [1, 2]. The seismic fragility of a pile was studied with different seismic demands in [3]. The nonlinear Winkler foundation model is widely used to study soil-pile and soil-pile-structure interactions using nonlinear dynamic analysis [4]. In [5], a comparison of soil-structure interaction and fix-base model effects on a structure's seismic fragility was presented.

A near-fault earthquake severely damages structures more than a far-fault one. This comparison was investigated in [6] through a numerical simulation of the seismic damage of arch bridges with three earthquake indicators: area intensity, energy rate, and cumulative absolute velocity. The demand/capacity ratio of an arch bridge pier is higher under near- than far-fault earthquakes [7]. In addition to [4], pushover analysis was used to study soil-pile and soil-pile-structure interactions in [8]. In a single pile, columns fail before pile foundations [9]. Soil permeability can be considered a complex property due to its influence on seismic fragility with different soil types [10]. In [11], the impact of the soil-pile interaction on the seismic fragility of wharf structures was investigated by comparing two systems: with and without soil-pile interaction. Most recent studies were based on the Winkler foundation model to study the seismic fragility of the Soil-Pile-Structure interaction (S-P-S). This model is a good instrument for investigating the seismic fragility of concrete bridge-soil systems using stepwise and LASSO regression [12]. In [13], the mitigation of pile group spacing on scour and liquefaction effects was studied.

The same results with [5] were shown in [14] considering a skewed bridge. In [15], the effect of irregular configuration and the stiffness of the substructure on the vulnerability of the bridge was shown. The soil-pile and soil-pile-structure interactions were investigated more comprehensively in [16]. The effects of the soil-structure interaction on the seismic fragility of a bridge were investigated in [17], considering the effects of wave passage. The selection of foundation type is an essential key for the construction of a superstructure and estimating its seismic fragility. The pile foundation is an improvement in superstructure performance compared to the shallow foundation [18]. The effects of soil stiffness and pile flexibility on the seismic fragility of the pile were assessed in [19] using finite element analysis. In addition to the effect of infrastructure parameters on the seismic fragility of the structure, there is the influence of the pier parameters, such as the higher-order mode of the pier bridge column that produces overestimated seismic demands of the pile foundation in terms of curvature and displacement [20]. The lateral performance of an eccentrically braced frame was investigated in [21]. The effectiveness of retrofitting a reinforced concrete structure was shown in [22]. In [23], the seismic performance of a base-isolated nuclear power plant structure was investigated taking into account near and far-fault earthquake influence.

This study investigated the effects of near- and far-fault earthquakes on the seismic fragility of a single-column pile, taking into account the soil-pile spring system's p - y curve using the Seismostruct software and incremental dynamic analysis.

II. NEAR AND FAR GROUND MOTION SELECTIONS

The main benchmark for selecting near- and far-fault earthquakes is the closest distance from the fault (Rjb) where the near-fault has an Rjb of less than 15Km [24]. This study used the records of earthquakes from [25]. The ground motions were characterized by a median of PGV/PGA equal to 113 for near- and 119 for far-fault. In Figure 1(a, b), the thin lines define the individual spectra, and the thick line defines the mean spectrum of near (NR) and far (FR) ground motions.

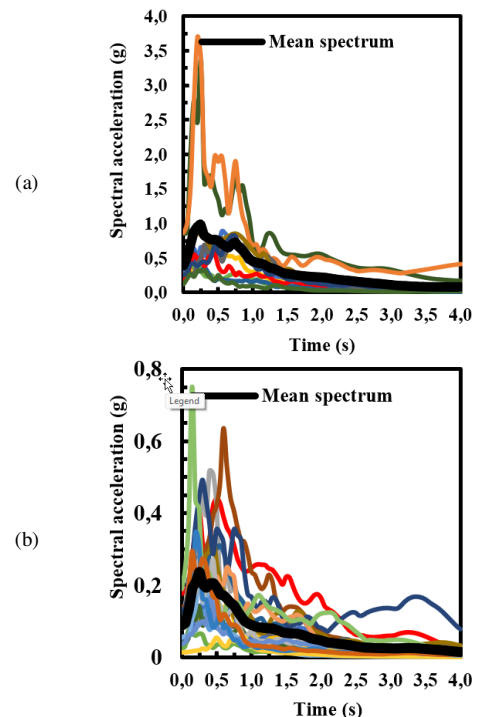


Fig. 1. Acceleration response spectra of (a) near-fault earthquakes, (b) far-fault earthquakes.

III. NUMERICAL MODELING OF SOIL-PILE INTERACTION

The Seismostruct software offers different concrete materials and steel reinforcing bars. The nonlinear Mander [26] and the Menegetto-Pinto models of steel reinforcing are shown in Figures 2 and 3. The modeling of the soil-pile interaction was based on the design of the p - y curve relationship: p is the soil reaction and y is the lateral deflection. The nonlinear Winkler foundation model (BNWF) [4] was employed, defined as multilinear curves. The structure was modeled using a 3D formulation, whereas the soil was modeled using a 1D formulation based on the reference p - y model as [4]:

$$p = 0.9p_u \cdot \tanh\left(\frac{k+z}{0.9p_u}y\right) \quad (1)$$

where k is the initial modulus of the subgrade reaction in soil and p_u is the ultimate bearing capacity.

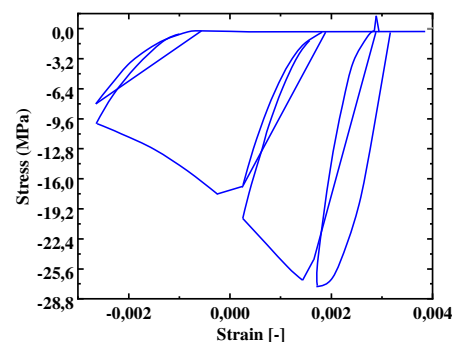


Fig. 2. Stress-strain curve of concrete mander material.

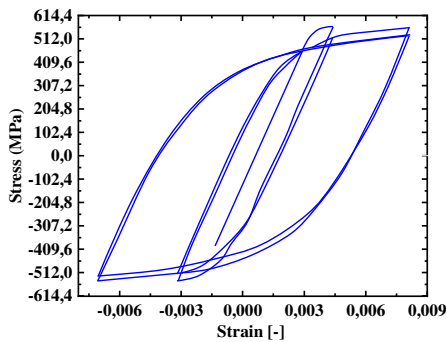


Fig. 3. Stress-strain curve of steel Menegetto-Pinto model.

The properties of each *p-y* curve derive from the parameters of homogeneous soil layers considering spring spacing of 0.5. Two different pile diameter deposits, each with two sand types, loose and dense, and three different masses were considered: 1500, 3000, and 4500kN. For simplification, an abbreviation is proposed concerning different models: LS for the loose sand model, DS for the dense sand model, and *d* for pile diameter, where $d=d_1=1.5\text{m}$ and $d=d_2=2\text{m}$. Two different heights (*H*) of piers, equal to 5 and 10m, were used. The pile length (*L*) was fixed at 30m as in [27]. The loose and dense sand had a friction angle of 30° and 45°, respectively. Figure 4 shows the soil-pile interaction model designed in Seismostruct software.

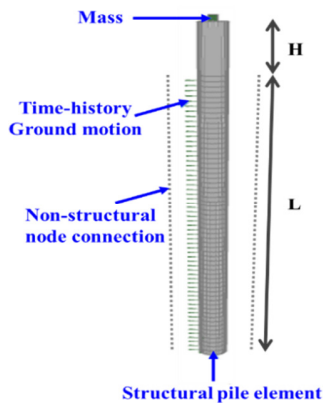


Fig. 4. Soil-pile spring interaction.

The calculation of the probability exceedance of a structure at a limit state is defined in (2), which is given by [15, 28-29]:

$$p\left(\frac{D}{PGA}\right) = \Phi\left(\frac{\ln(PGA) - \mu}{\sigma}\right) \quad (2)$$

where μ and σ are the mean and the standard deviation of the logarithmic of the peak ground acceleration when the pier reaches the threshold of performance level D at each limit state, and Φ is the standard normal cumulative distribution function. To estimate the probability of pier damage, the analysis procedure was (Figure 5):

1. Modeling of soil-pile interaction and vertical load value using Seismostruct software.
2. Define the drift value at each limit state of different models using nonlinear static analysis.

3. Select ground motion records (near- and far-fault earthquakes).
4. Generate the incremental dynamic analysis and find the median and standard deviation of the incremental dynamic analysis.
5. Drawing of seismic fragility curve.

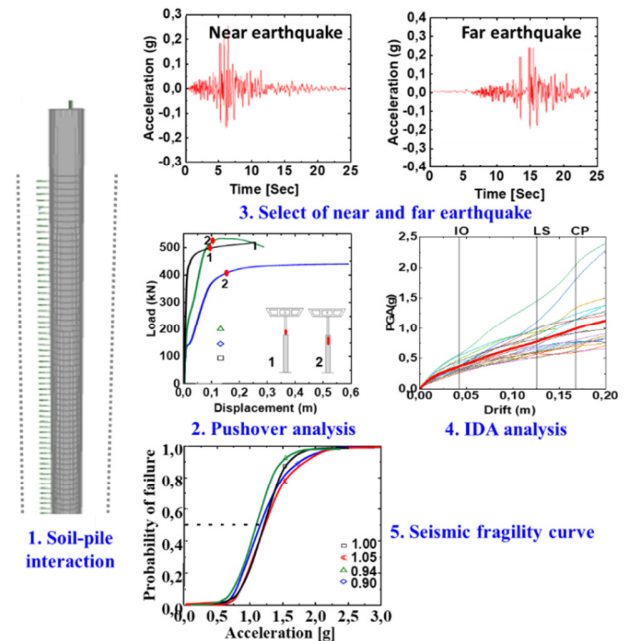


Fig. 5. Analysis procedure.

IV. RESULTS AND DISCUSSION

A. Limit States and Incremental Dynamic Analysis

Figure 6(a) shows the form of the incremental dynamic analysis example. The 20 thin lines define the individual incremental dynamic analysis and the thick red line defines its mean response. Figure 6(b) shows the comparison of the mean response. The mean response of the incremental dynamic analysis increases with mass center under the two ground motion types. After realizing the incremental dynamic analysis series for each model, their mean and standard deviation were calculated. The mean and standard deviation of incremental dynamic analysis in the case of pile diameter of 1.5 and 2.0 m, and $H=5\text{m}$ are shown in Tables I and II, respectively, and the mean value decreases with mass increase.

TABLE I. MEDIAN AND STANDARD DEVIATION VALUES OF IDA WITH PILE DIAMETER EQUAL TO 1.5 M

Mass (KN)		1500		3000		4500	
Earthquake type		Near	Far	Near	Far	Near	Far
Mean (μ)	Loose sand	0.94	1.03	0.38	0.37	0.23	0.22
	Dense sand	0.90	1.00	0.40	0.38	0.25	0.23
Standard deviation (σ)	Loose sand	0.36	0.37	0.32	0.35	0.28	0.31
	Dense sand	0.28	0.36	0.26	0.26	0.23	0.22

TABLE II. MEDIAN AND STANDARD DEVIATION VALUES OF IDA WITH PILE DIAMETER EQUAL TO 2M.

Mass (KN)		1500		3000		4500	
Earthquake type		Near	Far	Near	Far	Near	Far
Mean (μ)	Loose sand	1.73	1.70	0.82	0.76	0.50	0.47
	Dense sand	1.98	2.01	0.80	0.55	0.42	0.48
Standard deviation (σ)	Loose sand	0.36	0.32	0.32	0.32	0.30	0.32
	Dense sand	0.24	0.32	0.23	0.49	0.17	0.24

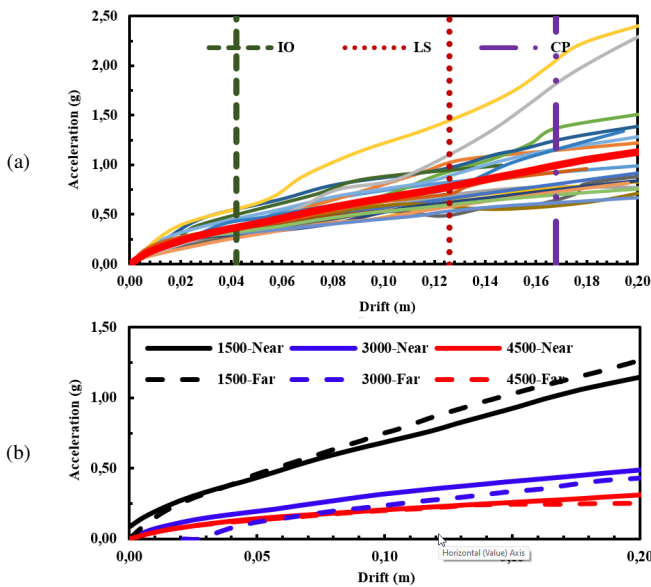


Fig. 6. (a) Incremental dynamic analysis under NR ground motion, (b) Example of mean response comparison of IDA.

B. Fragility Curves

Utilizing parameters from the mean and standard deviation of incremental dynamic analysis, and the standard normal cumulative distribution function (2), the fragility curves are expected and generated in the design figures for the collapse prevention state.

C. Effect of Mass

Depending on the variation of pier height (H), the results of the numerical simulation are classified into two parts: Figures 7 and 8 for H=5m and Figures 9 and 10 for H=10m. Figure 7(a) presents the seismic fragility of the concrete pier in case the pile is embedded in dense sand under a near-fault ground motion. This figure shows that when placing a different mass of 1500, 3000, and 4500kN, the pier structure needs a peak ground acceleration equal to 0.90, 0.40, and 0.25g, respectively, to exceed 50% of failure probability. These results show that the high mass needs a low Peak Ground Acceleration (PGA) to exceed 50% of failure probability under near-fault ground motion. The seismic fragility curves under far-fault ground motion show the same trend. All figures show similar trending results with a mass variation.

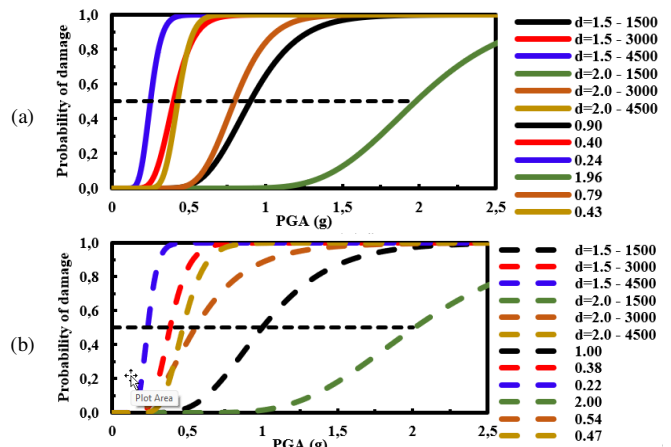


Fig. 7. Seismic fragility of pier with dense sand condition and H=5m: (a) Near (NR) ground motions, (b) Far (FR) ground motions.

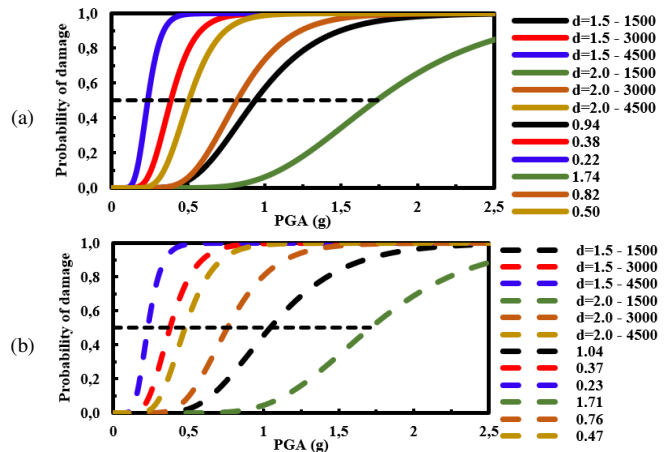


Fig. 8. Seismic fragility of a pier with loose sand conditions and H=5m: (a) Near (NR) ground motions, (b) Far (FR) ground motions.

D. Near and Far Fault Ground Motion Comparison

These results show that high mass needs a low PGA to exceed 50% of failure probability under near-fault ground motion. A comparison of seismic fragility curves under far-fault ground motion shows the same trend. Additionally, all Figures show similar trending results with mass variation. Figures 7 and 8 showed that the lower difference between PGA of near- and far-ground motion at 50% of failure probability in the case of H=5m are: LS-d1-3000, DS-d1-3000, LS-d1-4500, LS-d1-4500, LS-d2-4500. These models keep this most negligible difference value at complete failure probability (100%). The fundamental periods of the different models are 0.81, 0.69, 0.98, 0.85, and 0.56s, and their T_1/T_2 ratios were 2.89, 2.46, 2.88, 2.5, and 2.94, respectively.

On the other hand, some models have a slight difference at only 50% failure probability. The last figures show that in models presenting $R < 5\%$, the far-fault produced a higher failure probability than the near-fault ground motion due to its higher value of PGV/PGA. These models were LS-d2-1500 and LS-d2-3000 in the case of H=5m and DS-d2-1500 in the case of H=10m. The fundamental periods of these models were

0.41, 0.56, and 0.64s, and their T_1/T_2 ratios were 3.72, 3.5, and 1.82, respectively. These Figures showed a higher probability of failure of the pier structure in far-fault earthquakes than in near-ground motions, as observed in [31], while a higher probability of failure was presented in [23] in near-fault earthquakes in all events.

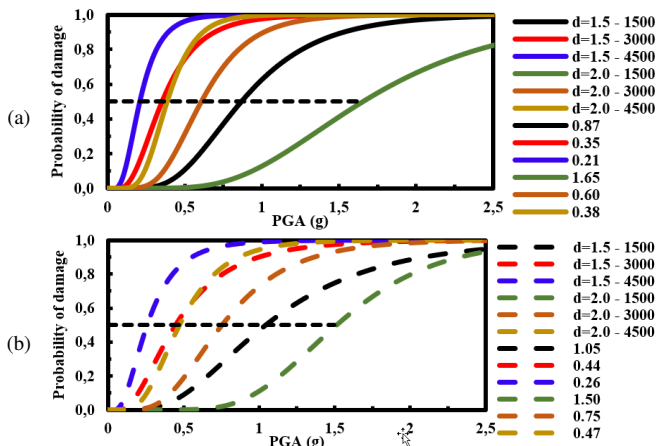


Fig. 9. Seismic fragility of pier with dense sand condition and H=10m: (a) Near (NR) ground motions, (b) Far (FR) ground motions.

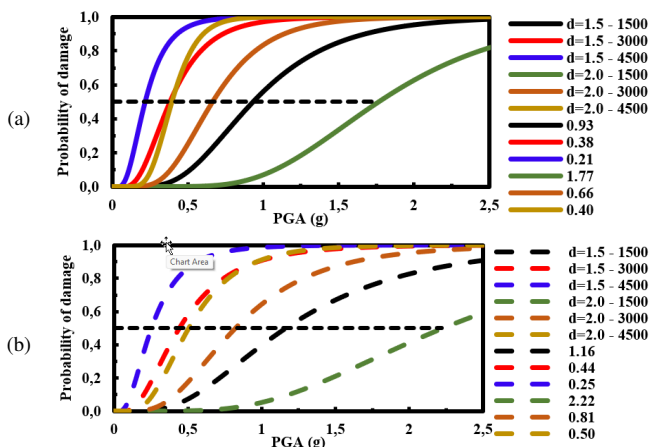


Fig. 10. Seismic fragility of pier with loose sand condition and H=10m: (a) Near (NR) ground motions, (b) Far (FR) ground motions.

V. CONCLUSIONS

This study compared the seismic fragility of a single concrete pier under near- and far-fault earthquakes. The effects of mass variation, closest ground motion type, and pile diameter were considered with two sand models, loose and dense. The seismic fragility of a concrete pier exceeded 50% and 100% of failure probability when placing a higher mass value at the pier end in all cases of pile section. The difference between the peak ground acceleration of near- and far-fault earthquakes at complete failure probability was less than 5% when the analysis modal conditions ($0.65s < T_1 < 1s$ and $2.4 < T_1/T_2$) were verified. The pier structure was highly affected by a higher value of PGV/PGA regardless of the near and far ground motions if one of two conditions was given:

$1 < T_1 < 0.65s$ or $T_1/T_2 < 2$. The higher difference between the peak ground acceleration of near and far earthquakes at complete failure probability was concluded if the two following conditions are presented together: $T_1 < 0.5s$ and $3 < T_1/T_2$.

REFERENCES

- [1] B. Aygün, L. Dueñas-Osorio, J. E. Padgett, and R. DesRoches, "Efficient Longitudinal Seismic Fragility Assessment of a Multispan Continuous Steel Bridge on Liquefiable Soils," *Journal of Bridge Engineering*, vol. 16, no. 1, pp. 93–107, Jan. 2011, [https://doi.org/10.1061/\(ASCE\)BE.1943-5592.0000131](https://doi.org/10.1061/(ASCE)BE.1943-5592.0000131).
- [2] A. R. Ghotbi, "Performance-based seismic assessment of skewed bridges with and without considering soil-foundation interaction effects for various site classes," *Earthquake Engineering and Engineering Vibration*, vol. 13, no. 3, pp. 357–373, Sep. 2014, <https://doi.org/10.1007/s11803-014-0248-7>.
- [3] A. R. Ghotbi, "Performance-based seismic assessment of a large diameter extended pile shaft in a cohesionless soil," *Earthquake Engineering and Engineering Vibration*, vol. 14, no. 1, pp. 177–188, Mar. 2015, <https://doi.org/10.1007/s11803-015-0015-4>.
- [4] A. Tombari, M. H. El Naggar, and F. Dezi, "Impact of ground motion duration and soil non-linearity on the seismic performance of single piles," *Soil Dynamics and Earthquake Engineering*, vol. 100, pp. 72–87, Sep. 2017, <https://doi.org/10.1016/j.soildyn.2017.05.022>.
- [5] S. P. Stefanidou, A. G. Sextos, A. N. Kotsoglou, N. Lesgidis, and A. J. Kappos, "Soil-structure interaction effects in analysis of seismic fragility of bridges using an intensity-based ground motion selection procedure," *Engineering Structures*, vol. 151, pp. 366–380, Nov. 2017, <https://doi.org/10.1016/j.engstruct.2017.08.033>.
- [6] N. Simos, G. C. Manos, and E. Kozikopoulos, "Near- and far-field earthquake damage study of the Konitsa stone arch bridge," *Engineering Structures*, vol. 177, pp. 256–267, Dec. 2018, <https://doi.org/10.1016/j.engstruct.2018.09.072>.
- [7] I. Mohseni, H. A. Lashkariani, J. Kang, and T. H. K. Kang, "Dynamic Response Evaluation of Long-Span Reinforced Arch Bridges Subjected to Near- and Far-Field Ground Motions," *Applied Sciences*, vol. 8, no. 8, Aug. 2018, Art. no. 1243, <https://doi.org/10.3390/app8081243>.
- [8] G. Houda, B. Tayeb, and D. Yahiaoui, "Key parameters influencing performance and failure modes for interaction soil–pile–structure system under lateral loading," *Asian Journal of Civil Engineering*, vol. 19, no. 3, pp. 355–373, Apr. 2018, <https://doi.org/10.1007/s42107-018-0033-4>.
- [9] M. Čosić, R. Folić, and B. Folić, "Fragility and reliability analyses of soil - pile - bridge pier interaction," *Facta universitatis - series: Architecture and Civil Engineering*, vol. 16, no. 1, pp. 93–111, 2018, <https://doi.org/10.2298/FUACE170420008C>.
- [10] L. Su et al., "Seismic fragility analysis of pile-supported wharves with the influence of soil permeability," *Soil Dynamics and Earthquake Engineering*, vol. 122, pp. 211–227, Jul. 2019, <https://doi.org/10.1016/j.soildyn.2019.04.003>.
- [11] L. Su, H. P. Wan, Y. Dong, D. M. Frangopol, and X.-Z. Ling, "Seismic fragility assessment of large-scale pile-supported wharf structures considering soil-pile interaction," *Engineering Structures*, vol. 186, pp. 270–281, May 2019, <https://doi.org/10.1016/j.engstruct.2019.02.022>.
- [12] Y. Xie and R. DesRoches, "Sensitivity of seismic demands and fragility estimates of a typical California highway bridge to uncertainties in its soil-structure interaction modeling," *Engineering Structures*, vol. 189, pp. 605–617, Jun. 2019, <https://doi.org/10.1016/j.engstruct.2019.03.115>.
- [13] X. Wang, A. Ye, and B. Ji, "Fragility-based sensitivity analysis on the seismic performance of pile-group-supported bridges in liquefiable ground undergoing scour potentials," *Engineering Structures*, vol. 198, Nov. 2019, Art. no. 109427, <https://doi.org/10.1016/j.engstruct.2019.109427>.
- [14] H. R. Noori, M. M. Memarpour, M. Yakhchalian, and S. Soltanieh, "Effects of ground motion directionality on seismic behavior of skewed bridges considering SSI," *Soil Dynamics and Earthquake Engineering*, vol. 127, Dec. 2019, Art. no. 105820, <https://doi.org/10.1016/j.soildyn.2019.105820>.

- [15] S. Soltanieh, M. M. Memarpour, and F. Kilanehei, "Performance assessment of bridge-soil-foundation system with irregular configuration considering ground motion directionality effects," *Soil Dynamics and Earthquake Engineering*, vol. 118, pp. 19–34, Mar. 2019, <https://doi.org/10.1016/j.soildyn.2018.11.006>.
- [16] K. Sekhri, D. Yahiaoui, and K. Abbache, "Inelastic Response of Soil-Pile-Structure Interaction System under Lateral Loading: A Parametric Study," *Jordan Journal of Civil Engineering*, vol. 14, no. 2, pp. 250–266, 2020.
- [17] O. M. O. Ramadan, S. S. F. Mehanny, and A. A.-M. Kotb, "Assessment of seismic vulnerability of continuous bridges considering soil-structure interaction and wave passage effects," *Engineering Structures*, vol. 206, Mar. 2020, Art. no. 110161, <https://doi.org/10.1016/j.engstruct.2019.110161>.
- [18] M. Ansari, M. Nazari, and A. K. Panah, "Influence of foundation flexibility on seismic fragility of reinforced concrete high-rise buildings," *Soil Dynamics and Earthquake Engineering*, vol. 142, Mar. 2021, Art. no. 106521, <https://doi.org/10.1016/j.soildyn.2020.106521>.
- [19] D. Forcellini, "Analytical Fragility Curves of Pile Foundations with Soil-Structure Interaction (SSD)," *Geosciences*, vol. 11, no. 2, Feb. 2021, Art. no. 66, <https://doi.org/10.3390/geosciences11020066>.
- [20] X. Chen, N. Xiang, and C. Li, "Influence of higher-order modes of slender tall pier bridge columns on the seismic performance of pile foundations," *Soil Dynamics and Earthquake Engineering*, vol. 142, Mar. 2021, Art. no. 106543, <https://doi.org/10.1016/j.soildyn.2020.106543>.
- [21] F. Abdelhamid, D. Yahiaoui, M. Saadi, and N. Lahbari, "Lateral Reliability Assessment of Eccentrically Braced Frames Including Horizontal and Vertical Links Under Seismic Loading," *Engineering, Technology & Applied Science Research*, vol. 12, no. 2, pp. 8278–8283, Apr. 2022, <https://doi.org/10.48084/etasr.4749>.
- [22] M. Saadi and D. Yahiaoui, "The Effectiveness of Retrofitting RC Frames with a Combination of Different Techniques," *Engineering, Technology & Applied Science Research*, vol. 12, no. 3, pp. 8723–8727, Jun. 2022, <https://doi.org/10.48084/etasr.4979>.
- [23] V. B. Tran, S. M. Nguyen, T. H. Nguyen, V. H. Nguyen, T. T. H. Doan, and D. D. Nguyen, "The Influence of Near- and Far-field Earthquakes on the Seismic Performance of Base-Isolated Nuclear Power Plant Structures," *Engineering, Technology & Applied Science Research*, vol. 12, no. 5, pp. 9092–9096, Oct. 2022, <https://doi.org/10.48084/etasr.5156>.
- [24] M. Bhandari, S. D. Bharti, M. K. Shrimali, and T. K. Datta, "Seismic Fragility Analysis of Base-Isolated Building Frames Excited by Near- and Far-Field Earthquakes," *Journal of Performance of Constructed Facilities*, vol. 33, no. 3, Jun. 2019, Art. no. 04019029, [https://doi.org/10.1061/\(ASCE\)CF.1943-5509.0001298](https://doi.org/10.1061/(ASCE)CF.1943-5509.0001298).
- [25] "PEER Ground Motion Database - PEER Center." <https://ngawest2.berkeley.edu/> (accessed Nov. 06, 2022).
- [26] J. B. Mander, M. J. N. Priestley, and R. Park, "Theoretical Stress-Strain Model for Confined Concrete," *Journal of Structural Engineering*, vol. 114, no. 8, pp. 1804–1826, Aug. 1988, [https://doi.org/10.1061/\(ASCE\)0733-9445\(1988\)114:8\(1804\)](https://doi.org/10.1061/(ASCE)0733-9445(1988)114:8(1804)).
- [27] N. Gerolymos, V. Drosos, and G. Gazetas, "Seismic response of single-column bent on pile: evidence of beneficial role of pile and soil inelasticity," *Bulletin of Earthquake Engineering*, vol. 7, no. 2, Apr. 2009, Art. no. 547, <https://doi.org/10.1007/s10518-009-9111-z>.
- [28] M. Miari and R. Jankowski, "Incremental dynamic analysis and fragility assessment of buildings founded on different soil types experiencing structural pounding during earthquakes," *Engineering Structures*, vol. 252, Feb. 2022, Art. no. 113118, <https://doi.org/10.1016/j.engstruct.2021.113118>.
- [29] X. Guo, Y. Wu, and Y. Guo, "Time-dependent seismic fragility analysis of bridge systems under scour hazard and earthquake loads," *Engineering Structures*, vol. 121, pp. 52–60, Aug. 2016, <https://doi.org/10.1016/j.engstruct.2016.04.038>.
- [30] D. Vamvatsikos and C. A. Cornell, "Incremental dynamic analysis," *Earthquake Engineering & Structural Dynamics*, vol. 31, no. 3, pp. 491–514, 2002, <https://doi.org/10.1002/eqe.141>.
- [31] A. Mosleh, M. S. Razzaghi, J. Jara, and H. Varum, "Seismic fragility analysis of typical pre-1990 bridges due to near- and far-field ground motions," *International Journal of Advanced Structural Engineering (IJASE)*, vol. 8, no. 1, pp. 1–9, Mar. 2016, <https://doi.org/10.1007/s40091-016-0108-y>.